frontiers | Frontiers in Mechanical Engineering

ORIGINAL RESEARCH
published: 08 April 2022
doi: 10.3389/fmech.2022.867685

Effect of Calcium Sulphate Pre-crosslinking on Rheological Parameters of Alginate Based Bio-Inks and on Human Corneal Stromal Fibroblast Survival in 3D Bio-Printed Constructs

Anastassia Kostenko[1], *Stephen Swioklo*[2] *and Che J. Connon*[1]*

[1]Biosciences Institute, Newcastle University, Newcastle Upon Tyne, United Kingdom, [2]Atelerix Ltd., Newcastle Upon Tyne, United Kingdom

OPEN ACCESS

Edited by:
Damien Lacroix,
The University of Sheffield,
United Kingdom

Reviewed by:
Shaoting Lin,
Massachusetts Institute of Technology, United States
Mahdi Bodaghi,
Nottingham Trent University,
United Kingdom

***Correspondence:**
Che J. Connon
che.connon@newcastle.ac.uk

Specialty section:
This article was submitted to Biomechanical Engineering, a section of the journal Frontiers in Mechanical Engineering

Received: 01 February 2022
Accepted: 09 March 2022
Published: 08 April 2022

Citation:
Kostenko A, Swioklo S and Connon CJ (2022) Effect of Calcium Sulphate Pre-crosslinking on Rheological Parameters of Alginate Based Bio-Inks and on Human Corneal Stromal Fibroblast Survival in 3D Bio-Printed Constructs. Front. Mech. Eng 8:867685. doi: 10.3389/fmech.2022.867685

The principle of three-dimensional (3D) bio-printing involves integration of biomaterials, live cells and controlled motor systems for creating complex biomimetic constructs. Bio-ink is one of the most important components in the process of 3D bio-printing and needs to be sufficiently viscous to be dispensed as a free-standing filament but be biocompatible to maintain cell viability and function. Alginate has been used widely for 3D bio-printing due to its biocompatibility, tunable properties, rapid gelation, low cost, and ability to be functionalized to direct cell behavior. By tuning the physiochemical parameters of alginate-based bio-inks, such as viscosity, improvements in print resolution, fidelity and growth characteristics of encapsulated cells can be achieved. This study aimed to improve the printability of low concentration alginate bio-inks by utilizing calcium sulphate (CaSO4) pre-crosslinking. A variety of alginates, differing in their viscosity, molecular weight and b-D-mannuronate and α-L-guluronate residues were investigated by wet spinning and bio-printing. Rheological and structural properties of pre-crosslinked alginates were characterized with the aim of mitigating the resolution problems associated with the use of low percentage alginate bio-inks, more favorable for maintaining cell viability. Pre-crosslinking produced a significant effect on viscosity of biomaterials improving their suitability for the bio-printing process and influencing the final resolution of the printed structure. Medium viscosity high b-D-mannuronate containing alginate (MVM) showed the highest degree of viscosity change compared to the control ($p < 0.0001$; n = 6), assessed by single value viscometry analysis and shear rheology, after pre-crosslinking and was subsequently used in experiments with cells. The survival of human corneal stromal fibroblasts (CSFs) was assessed using CellTiterGlo metabolic assay and confirmed with Calcein acetoxymethyl and Ethidium homodimer -1 live/dead staining in pre-crosslinked alginate fibers and bio-printed lattices. Encapsulation of CSFs in pre-crosslinked alginate-based bio-inks did not have a detrimental effect on CSF viability compared to the non-pre-crosslinked control over 7 days under standard cell culture conditions ($p > 0.05$, n = 3).

Overall, printability of low percentage alginate bio-inks was improved by pre-crosslinking without affecting the biocompatibility of the bio-inks.

Keywords: alginate, scaffold, corneal stromal fibroblasts, 3D bioprinting, rheology

INTRODUCTION

In the last decade, interest and progress in the field of three-dimensional (3D) bio-printing has increased enormously. The technology presents huge potential in regenerative medicine, drug discovery, tissue engineering, novel model development to study disease pathogenesis and drug toxicity and allows for development of intricate tissue structures to mimic native organs (Murphy and Atala, 2014; Mandrycky et al., 2016; Donderwinkel et al., 2017; Murphy et al., 2020). 3D bio-printing comprises of a fusion of different disciplines, including bioengineering and biomaterial science, computer-aided design, developmental biology, cytobiology, molecular biology and clinical medicine. The principle of 3D bio-printing integrates biomaterials, live cells, and controlled motor systems for creating complex structures (Donderwinkel et al., 2017). Hence, fabrication of intricate structures with controlled porosity, permeability and mechanical properties is possible. Different cell types, biomolecules and biomaterials can be placed together in desired concentrations and specifically positioned generating biomimetic constructs. This layering of biocompatible scaffolds, factors and cells aspires to recapitulate native biologic tissue and has tremendous potential for the future of drug discovery and regenerative medicine. 3D bio-printed structures with programed cells will be able to not only mimic highly organized tissues but can also provide new functions as living responsive materials and devices (Liu et al., 2018).

The most common type of 3D bio-printing is extrusion-based 3D bio-printing. Usually, extrusion-based bio-printers have multiple print heads to be able to incorporate multiple biomaterials in one printed construct. The benefit of this is the ability to create scaffolds with regional differences in cell types and densities, specific positioning of growth factors and signaling molecules as well as option to incorporate a variety of biomaterials into the same construct (Gillispie et al., 2020). However, one of the biggest drawbacks of the technique besides resolution is exposure of encapsulated cells to shear stress when the cells are in the syringe and when extruded through the nozzle during the printing process, as the cell-laden bio-ink is dispensed by creating a pressured environment in a pneumatic or mechanical system. This pressure, necessary for extrusion to take place, can decrease cell viability and subsequent cell function after printing, which affects the overall cell survival in the construct. Thus, one of the greatest challenges in the field of 3D bio-printing remains the development and selection of a suitable bio-ink. There are many parameters that a successful bio-ink needs to possess, for example adequate printability, which requires the bio-ink to be sufficiently viscous to be dispensed as a free-standing filament, have a shear-thinning formulation, have appropriate strength and stiffness to maintain structural integrity and shape fidelity after bio-printing, yet be compliant enough to be extrudable and not clog the nozzle (Chung et al., 2013). To create a hydrogel-based scaffold, crosslinking steps need to enhance the mechanical strength of the bio-ink as well as aid in inter-layer adhesion of the extruded layers. Requirements of a scaffold include robust mechanical strength combined with ability to support cell viability and function, biocompatibility, and favorable biodegradation properties. In the field of tissue engineering, it is also important for the bio-printed scaffolds to be sterile, cytocompatible and promote cell-matrix interaction to induce tissue formation (Li et al., 2021).

Hydrogels are hydrophilic polymers and are favored biomaterials in bio-ink development. Hydrogels generally exhibit high biocompatibility and non-immunogenicity, and their hydrated network structure creates an environment permissive to the encapsulation of cells and other biomaterials for the purpose of subsequent 3D bio-printing. Hydrogels are composed of crosslinked hydrophilic polymers that absorb large amounts of water and are commonly used in tissue engineering applications due to their low cytotoxicity and structural similarity to native extracellular matrix (ECM). Hydrogels that are used as bio-inks can be either natural or synthetic, with each having their own advantages and disadvantages. Most common examples of synthetic bio-inks include poly (ethylene glycol)s (PEGs), pluronics, polyacrylamide, poly (2-hydroxyethyl lmethacrylate) (PHEMA) and many others. Natural bio-inks include alginate, gelatin, collagen, agarose, chitosan, cellulose, dextran, fibrin, gellan gum, and hyaluronic acid. Natural hydrogels can contain inherent ligands, which facilitate cell adhesion and differentiation and are often isolated from ECM components (e.g. gelatin and collagen). The benefits of natural hydrogels are improved bioavailability and biocompatibility, synthetic hydrogels are cheaper, have no batch-to-batch variability and are easily tunable in terms of degradation parameters (Gillispie et al., 2020). The bio-fabrication window for rational design of bio-inks also needs to be considered, as it requires compromise between printability and biocompatibility with minimal degree of cytotoxicity being an ideal bio-ink for 3D bio-printing (Malda et al., 2013; Chimene et al., 2016; Gopinathan and Noh, 2018; Fontes and Marcomini, 2020). Besides the mechanical properties, the material used as a bio-ink preferably needs to provide a degree of protection from shear stress to the encapsulated cells to maintain their viability during the 3D bio-printing process as well as facilitate cell survival post-print (Lee and Mooney, 2012; Kyburz and Anseth, 2015; Fontes and Marcomini, 2020; Mancha Sánchez et al., 2020; Ramiah et al., 2020; Unagolla and Jayasuriya, 2020; Nie et al., 2020).

The bio-ink of choice in this paper is the highly biocompatible polysaccharide of natural origins—alginate. Alginate is a water soluble, linear anionic polysaccharide that can be obtained from the cell wall of brown algae of the class Phaeophyceae with

sodium hydroxide producing sodium alginate. Species that can yield alginate include *Laminaria hyperborea, Laminaria digitata, Laminaria japonica, Ascophyllum nodosum, and Macrocystispyrifer* (Lee and Mooney, 2012). Numerous applications in biomedical science and tissue engineering use alginate as a biomaterial due to its favourable properties such as low cost, ease of gelation with divalent cations, biocompatibility, mechanical stability, lack of cytotoxicity and immunogenicity as well as structural similarity to the native extracellular matrix. Alginate can be engineered and fine-tuned to suit the desired application, be it in the fields of 3D bio-printing, drug discovery or delivery or wound healing approaches. In addition, alginate is a highly extrudable material and is commonly used as a bio-ink in 3D bio-printing, either on its own or in combination with other bioactive components by many researchers in the field (Elkayam et al., 2006; Ahn et al., 2012; Fedorovich et al., 2012; Poldervaart et al., 2013; Wüst et al., 2014; Tabriz et al., 2015; Wang et al., 2015; Freeman and Kelly, 2017; Schütz et al., 2017; Gao et al., 2018; Lee et al., 2020). Moreover, Gasperini et al. suggest that the wide pore size distribution of alginate (5–200 mm) enables large molecular diffusion in and out of the gel, which explains the frequent use of alginate as a drug or growth factor delivery system (Gasperini et al., 2015). The molecular structure of alginate is composed of unbranched binary copolymers of a-L-guluronic acid (G block) and (1–4)-linked b-D-mannuronic acid (M block) residues as monomers with different sequential occurrence (Stokke et al., 2000; Draget et al., 2006; Bishop et al., 2017; Urbanova et al., 2019). Both the G and M blocks can be arranged in a homopolymeric, consecutive manner (either GGGG or MMMM) or alternating manner (GMGM). This internal arrangement and ratio of M and G blocks and the overall length of the polymer vary depending on the source of extraction and influence the physiochemical properties of the polymer. The process of crosslinking can be achieved when the carboxyl group of α-l-guluronic acid comes into contact with a divalent cation forming a chelate structure with the metal ion that has been termed the "egg-box" junction. This specific and strong interaction between pairs of 21 helical chains with the calcium ions located between them induces chain-chain association responsible for gel formation (Braccini and Pérez, 2001; Lee and Mooney, 2012; Merakchi et al., 2018). The most conventional choice of ionic crosslinker of alginate is Calcium Chloride ($CaCl_2$), due to its high solubility in aqueous solutions and rapid gelation reaction. Calcium carbonate ($CaCO_3$) and calcium sulphate ($CaSO_4$) are also popular crosslinking options, yet due to their reduced solubility in aqueous solutions the gelation of alginate is a lot more gradual. The choice of crosslinker can significantly affect the physiological parameters and mechanical properties of resulting bio-ink (Ck and Px, 2001; Lee and Mooney, 2012; Freeman and Kelly, 2017).

In this study, this slower gelation mechanism of $CaSO_4$ has been utilized to produce a pre-crosslinked alginate-based bio-ink able to support the viability of human corneal stromal fibroblasts (CSFs) in standard cell culture conditions. A variety of commercially available alginates differing in their M:G ratio have been tested. The change in viscosity as well as rheological parameters of the produced pre-crosslinked bio-inks and controls were characterized extensively and are described in more detail in the results section. The pre-crosslinked alginate-based bio-inks were also characterized in terms of diameter of fibers they can produce by wet spinning as well as used to encapsulate CSFs and 3D bio-printed in a shape of a lattice. The viability and metabolic activity of CSFs in the construct was assessed at different times in standard cell culture conditions. The overall aim of the study was to identify if pre-crosslinking of low percentage alginate-based bio-inks with $CaSO_4$ is a useful strategy to improve bio-ink printability without having a detrimental effect on cell survival.

MATERIALS AND METHODS

Alginate Preparation

To produce 2.4% (w/v) aqueous alginate stock solutions, sodium alginate powders differing in the content of mannuronic acid (M) and guluronic acid (G) residues and molecular weight (Mw) were obtained from Pronova (Novamatrix, Sandvika, Norway) weighed out and dissolved in ddH2O. The alginates tested included Very Low Viscosity high G content (VLVG), Low Viscosity High G content (LVG), Medium Viscosity High G content (MVG), Very Low Viscosity high M content (VLVM), Low Viscosity high M content (LVM), Medium Viscosity high M content (MVM). The molecular weights of the used alginates were <75 kDa for VLVG and VLVM, 75–200 kDa for LVG and LVM, >200 for MVG and MVM. The contents of mannuronic acid and guluronic acid residues of VLVM, LVM and MVM alginates were 50:50 G:M, VLVG, LVG and MVG were 60:40 G: M. To facilitate complete alginate solubilisation the solution was vortexed and left on continuous shaking for 24 h at room temperature. 2.4% alginate stock solutions were then further diluted with ddH2O with or without the addition of $CaSO_4$ to form the final concentration of 1.2% alginate, which has then been used in all following experiments.

Calcium Chloride Preparation for Post-crosslinking of the Bio-Ink

A stock solution of $CaCl_2$ (100 mM) (Sigma Aldrich, Gillingham, United Kingdom) was produced by weighing out the salt and dissolving it in ddH2O at room temperature. This solution was used to post-crosslink the pre-crosslinked or control gels by either directly extruding the alginate into a CaCl2 bath in the case of wet spinning or depositing 0.2 ml of post-crosslinking CaCl2 solution directly onto the 3D bio-printed constructs after printing.

Pre-Crosslinking of Alginate With $CaSO_4$

Stock solution (2.4%) of alginate was mixed in a 1:1 ratio with ddH2O containing 0.001 M Calcium Sulfate ($CaSO_4$) (ACROS, Thermo Fisher Scientific, Loughborough, United Kingdom) producing the final concentration of 1.2% pre-crosslinked alginate. The alginate $CaSO_4$ mixtures were mixed 50 times using the dual syringe method and left to cure at RT for 3 h prior to being evaluated. Following curing and prior to use the solutions were briefly centrifuged to remove air bubbles created by the mixing process.

Collagenase Enzyme Digestion of Human Corneal Stromal Fibroblasts

Human corneal rings were kindly donated by Professor Francisco Figueiredo, Consultant Ophthalmologist at the Newcastle upon Tyne Hospitals NHS Foundation Trust and Professor of Ophthalmology at Newcastle University. The human donor ages of the corneal rings were between 65 and 80 years old with no prior history of corneal disease. The corneal center was removed using a biopsy punch (diameter = 0.8 mm) to separate the central and the limbal region of the cornea. A scalpel was then used to finely cut the central and the limbal regions of the cornea in separate Petri dishes. For the collagenase digestion to take place, 2 g/L of collagenase type-1 enzyme (Invitrogen, Thermo Fisher Scientific, Loughborough, United Kingdom) were solubilized in DMEM/F12 culture medium (Sigma Aldrich, Gillingham, United Kingdom) containing 10% fetal bovine serum (FBS) (Biosera, Heathfield, United Kingdom) and added to the finely cut corneal pieces. The mixture was then placed in a rotisserie rotator for 5 h of continuous rotation at 37°C and 5% CO_2. Afterwards, the mixture was filtered using a cell strainer to separate the cells from debris and the isolated CSFs were placed in T25 tissue culture flasks (Greiner Bio-One, Stonehouse, United Kingdom) and cultured normally under standard cell culture conditions.

Human CSF Culture

Human CSFs used in this project were extracted from donated human corneas by collagenase enzyme digestion. The components necessary for making the complete CSF serum medium include: Basal medium—Dulbecco's Modified Eagle Medium/Nutrient Mixture F-12 GlutaMAXTM (DMEM/F12) (Sigma Aldrich, Gillingham, United Kingdom), 10% Foetal Bovine Serum (Biosera, Heathfield, United Kingdom), 5% Penicillin/Streptomycin (Life Technologies, Thermo Fisher Scientific, Loughborough, United Kingdom). After plating to T175 flasks, CSFs were kept in a humidified incubator at 37°C with 5% CO2. The cells were monitored regularly and passaged every 2–3 days until reaching 70–80% confluence. In all experiments cell passages between 1 and 10 were used.

Human CSF Encapsulation in Alginate

After expansion of CSFs to 70–80% confluency in normal culture conditions, the cells were detached using TrypLE enzyme (Gibco brand, Thermo Fisher Scientific, Loughborough, United Kingdom), then re-suspended in 1 ml of complete medium, counted using Trypan blue and automated cell counter (Countess II FL, Invitrogen, Thermo Fisher Scientific, Loughborough, United Kingdom) and upon determining the desired cell number, added directly to the alginate gel. Cell density within alginate gels was 1 million cells per mL of gel.

Wet Spinning

To investigate the effect pre-crosslinking has on the diameter of the produced alginate fibers, a version of wet spinning was used. Pre-crosslinked alginates and non-crosslinked controls at 1.2% were extruded using the Legato 101 syringe pump (kd Scientific, Holliston, United States) at the rate of 1 ml/min into 10 ml of 0.1 M $CaCl_2$ solution through a 30G polytetrafluoroethylene (PTFE) lined needle, Fisnar, 0.006″ I.D. 0.5", Teflon lined Tip (Intertronics, Kidlington, United Kingdom) for ionic crosslinking to take place. The fibers were crosslinked for 10 min prior to being transported into Hanks' Balanced Salt Solution (HBSS) without calcium, magnesium and phenol red (Gibco brand, Thermo Fisher Scientific, Loughborough, United Kingdom), containing wells and washed for 2 min prior to analysis of fiber diameter. The fibers were photographed using Cytation™ 1Cell Imaging Multi-Mode Reader (Agilent BioTek, Harwell, United Kingdom) where the diameter of the produced fibers was measured using the Gen 5 3.08 Image Analysis Software. The same procedure was performed with the addition of CSFs to assess their viability in control and pre-crosslinked fibers. All solution preparations and experiments were performed at room temperature.

3D Bio-Printing

Acellular pre-crosslinked alginates and controls were used as bio-inks and bio-printed through a 30G PTFE lined needle (Fisnar, 0.006 "I.D. 0.5", Teflon lined Tip) at 45–65 kPa using the CELLINK INKREDIBLE bio-printer (CELLINK, Brighton, United Kingdom) in a shape of a lattice with the addition of 0.1 M $CaCl_2$ for 2 min as a post-crosslinking step on top. Video of the bio-printing process to produce a lattice is available in **Supplementary Materials**. Subsequently the lattices were photographed using Cytation™ 1Cell Imaging Multi-Mode Reader and line diameters of the constructs were measured using the Gen 5 3.08 Image Analysis Software. CELLINK alginate-based bio-ink (CELLINK, Brighton, United Kingdom) was bio-printed in a similar manner to act as a positive control. Upon selection of pre-crosslinked MVM alginate as the bio-ink of choice, CSFs were seeded into the pre-crosslinked alginate gels, gently mixed up and down with a syringe to make sure CSFs are evenly distributed throughout the gel and bio-printed. Crosslinking solution (0.1 M $CaCl_2$) was added drop wise on top of the cell-laden constructs and left to crosslink for 2 min. Crosslinking time was changed to 2 min because of the smaller size of the lattice compared to the wet spun fiber. The crosslinking solution was removed, and the cell laden constructs were washed with the complete cell culture medium for 5 min. The medium was then removed and substituted with fresh cell culture medium. The viability of cells immediately after printing (day 0) was assessed and the cell laden constructs were placed in a humidified incubator at 37°C with 5% CO_2 and cultured under standard cell culture conditions. The same procedure was performed with CSF laden CELLINK control bio-ink to compare the metabolic activity of CSFs in CELLINK and pre-crosslinked MVM alginate. To demonstrate the ability of the pre-crosslinked MVM bio-ink to maintain its shape as a free-standing filament upon extrusion a ring shape was also 3D bio-printed without the addition of post-crosslinking $CaCl_2$ solution, photograph and video of the process are available in **Supplementary Materials**.

Assessment of Rheology and Viscometry on $CaSO_4$ Pre-crosslinked Alginate Bio-Inks

Rheological measurements were performed on all 1.2% alginate solutions, controls and pre-crosslinked with CaSO4. All the samples have been briefly centrifuged to remove the air bubbles and the influence of the centrifugation step on the mechanical properties of the gels was assessed and compared to non-centrifuged samples with no significant difference (data not shown). The respective test samples were dispensed on the bottom plate geometry and finally trimmed, once the upper geometry was in place. Each experiment was conducted six times and the mean and standard deviation (SD) were calculated and are presented. All samples were studied by determining the linear viscoelastic region (LVER), Viscometry Single Value at shear frequency of 1 Hz, viscometry ramp over a range of shear frequencies, oscillation amplitude sweep and oscillation frequency sweep. Kinexus pro + rotational rheometer (Malvern instruments Ltd., Malvern, United Kingdom) was used to obtain rheological data as well as viscometry measurements. Parallel plate geometry (CP1/60 60 mm diameter with a 1 mm gap) with controlled shear strain was used. All measurements were performed at 25°C and rSpace software was used for data analysis. Rheological data including the shear elastic modulus G′, shear loss modulus G", and loss tangent tan(δ) was collected from the oscillation frequency sweep, conducted over a frequency range 0.1–10 Hz.

Viability Staining With (CAM/Ethd-1) Staining

Calcein acetoxymethyl (CAM), live stain, and ethidium homodimer-1 (Ethd-1), dead stain, were used to determine cellular viability. Both dyes were obtained from Thermo Fisher Scientific, Loughborough, United Kingdom. The staining protocol used a 1/1,000 concentration of CAM or Ethd-1 diluted in HBSS (Gibco, Thermo Fisher Scientific, Loughborough, United Kingdom. An incubation step of 20 min took place whereby the plate was placed in the dark at room temperature followed by a wash with HBSS prior to imaging and counting using Cytation™Cell Imaging Multi-Mode Reader.

Assessment of Cellular Metabolism With CellTiterGlo Assay

The CellTiterGlo assay (CTG) (Promega, Hampshire, United Kingdom) determines the number of viable cells in culture by quantifying ATP, which indicates the presence of metabolically active cells. The viability of CSFs was assessed on the day of bio-printing after the constructs were placed in standard CSF culture medium for 5 h. Cell culture media (150 µL) from the constructs was added to 150 µL of CTG reagent and mixed by pipetting up and down 10 times to ensure homogenous mixing. Triplicates of 100 µL per sample were then loaded into an opaque, white, flat bottom 96 well plate (Corning® 96 Well Solid Polystyrene Microplate, Deeside, United Kigdom). The plate was shaken on an orbital shaker for 10 min and the luminescence was measured using Cytation™Cell Imaging Multi-Mode Reader with the integration time of 0:01.00 MM:SS.ss and gain of 135. The same procedure was utilized on all subsequent time points—day 1 and day 7.

RESULTS AND DISCUSSION

The Effect of Alginate Molecular Weight, G:M Ratio and Pre-crosslinking on the Hydration and Swelling Properties of Bio-Inks

To understand the effect of molecular weight (Mw), G:M ratio and pre-crosslinking on the hydration and swelling of alginate fibers control or pre-crosslinked alginates were wet spun using a syringe pump into a post-crosslinking $CaCl_2$ bath where they were crosslinked for 10 min prior to performing weight measurements. The fibers were removed from the crosslinking bath, gently tapped onto filter paper to remove excess liquid and weighed in the hydrated state (wet weight). The results are presented in **Figure 1Ai** for control alginates and (**Figure 1Aii**) for pre-crosslinked alginates. After overnight drying in a non-humidified incubator at 40°C the fibers were weighed again to obtain the dry weight. The results are presented in **Figure 1Bi** for control alginates and (**Figure 1Bii** for pre-crosslinked alginates. All experiments were performed six times. No significant differences in terms of wet or dry weight were observed between different types of alginates, indicating that in this study and at concentrations tested hydration was not affected by the differences in molecular weight and M:G ratio. No significant differences were observed between the wet weights of control and pre-crosslinked alginates, indicating that pre-crosslinking of alginate fibers with $CaSO_4$ at the concentration tested (0.001 M) does not affect the hydration capacity of alginate fibers, thus indicating that pre-crosslinking should have no effect on the eventual biocompatibility with cultured cells. The degree of hydration was calculated using the formula Hydration % = (average wet weight-average dry weight)/average wet weight x100. Hydration of control alginate fibers is presented in **Figure 1Ci** and hydration of pre-crosslinked alginate fibers is presented in (**Figure 1Cii**). Both the control alginates and the pre-crosslinked alginates showed a high degree of hydration of above 96% for all alginates tested. No significant differences between the dry weights of different alginate types or control and pre-crosslinked alginates were observed. Based on the weight measurements the degree of swelling of the alginate fibers could be calculated using the formula Swelling % = (wet weight—dry weight)/dry weight x100. Swelling properties of the bio-inks are not critical for the 3D bio-printing process, thus the results are presented in **Supplementary Materials Figure S1Ai** for control alginate fibers and **Supplementary Materials Figure S1Aii** for pre-crosslinked alginates fibers. A one-way ANOVA and parametric tests were performed for statistical analysis and no significant differences were found in terms of hydration and swelling of all the alginates tested, controls and pre-crosslinked.

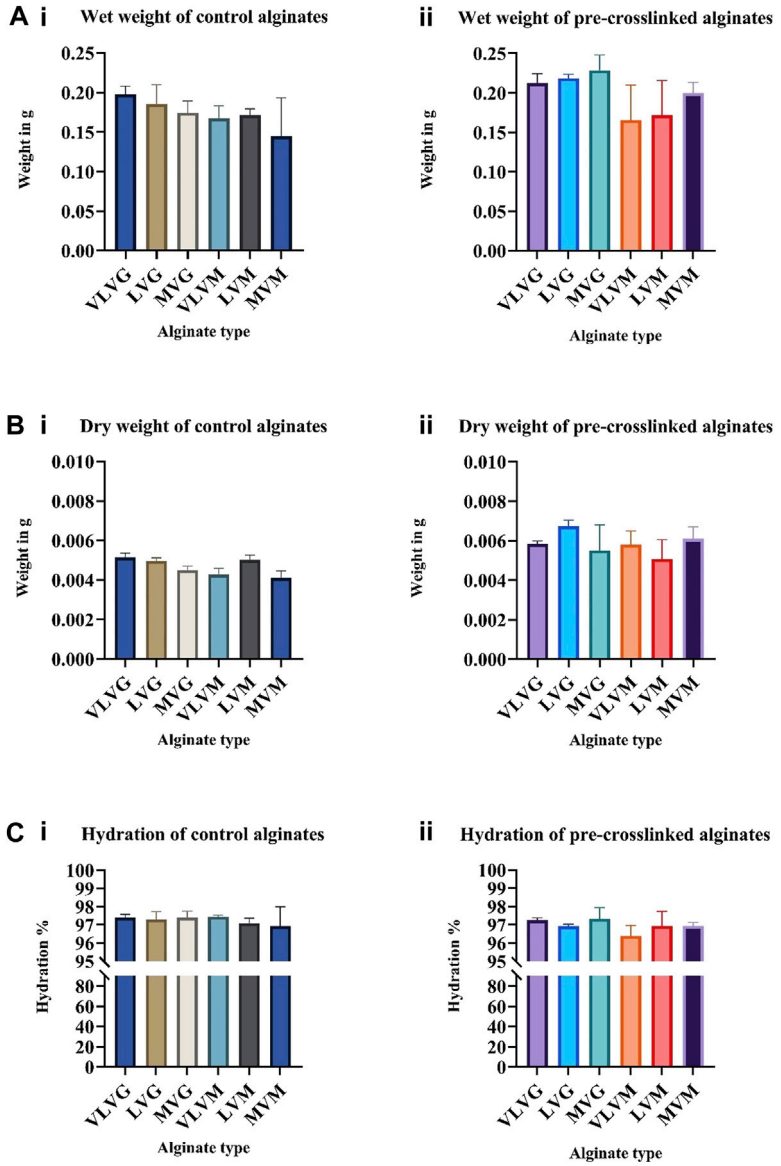

FIGURE 1 | The effect of alginate molecular weight, G:M ratio and pre-crosslinking on the hydration properties of bio-inks. Fibers were formed by wet spinning before assessing wet weight and dry weight of control **(Ai,Bi)** and pre-crosslinked **(Aii,Bii)** alginate fibers. Weight values were used to calculate hydration % of control alginate fibers **(Ci)** and pre-crosslinked alginate fibers **(Cii)**. Values are expressed as mean ± SD from six separate experiments.

It was unexpected to see no change in degree of hydration of alginate fibers differing in their molecular weight, as previous studies have reported an increase in degree of hydration of alginates with increasing Mw due to hydrogen bonding, hydrophobic and electrostatic forces and microstructure of the gel (Xiong and Blanchard, 1993; Chen et al., 2006; Ma et al., 2013; Yao et al., 2018). An increase in the prevalence of hydrophilic groups and charged groups is expected in alginates with a greater Mw, which would lead to more interaction with water and subsequent higher physical entrapment of water in the gel network. Yao et al., 2018 observed an increase in water holding content in composite myosin-alginate gels that utilized higher Mw alginates (Mw = 4,640 kDa), yet no significant difference was observed between low Mw alginates (Mw = 2,660 kDa) and medium Mw alginates (Mw = 3,890 kDa) according to the authors. The concentration of alginate assessed in the study by Yao *et al.* ranged from 0 to 0.5%. The reported water holding capacity of myosin-alginate gels ranged between 92% in low and medium Mw alginates and 94% in high Mw alginate. In this study, the concentration of alginates was higher (1.2%), yet the molecular weights of alginates used were a lot lower (<75 kDa, 75–200 kDa and >200 kDa) than in the study by Yao *et al.* which could be the reason for no significant differences in terms of hydration. This suggests that critical alginate concentration and molecular weight exist whereby differences in hydration can be observed, whereas in this study

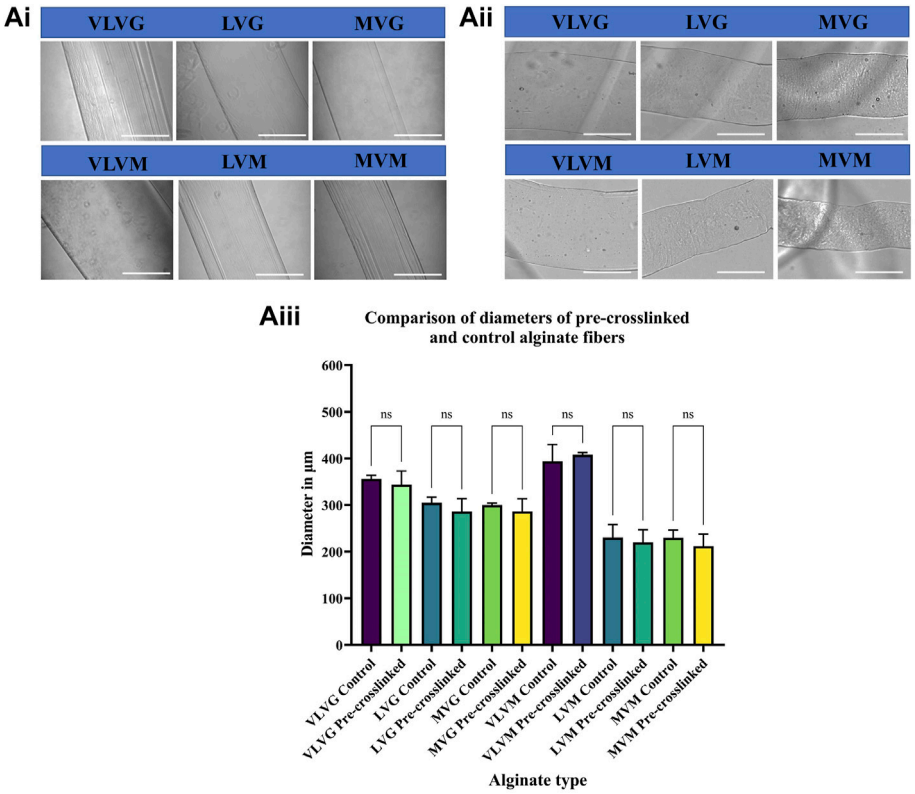

FIGURE 2 | The effect of alginate molecular weight, G:M ratio and pre-crosslinking on the diameter of wet spun alginate fibers. Fibers were formed by wet spinning prior to being imaged. Control alginate fibers are presented in **(Ai)**, pre-crosslinked alginate fibers are presented in **(Aii)**, comparison of diameters of pre-crosslinked and control alginate fibers is presented in **(Aiii)**. Values are expressed as mean ± SD from six separate experiments.

the degree of hydration has reached its maximum capacity. Additionally, it was unexpected to see no significant difference in terms of swelling capacity of high G residue containing alginates and high M residue containing alginates, as it has been previously reported in wound exudate studies that high M residue containing alginates have increased absorbency. This is due to stronger calcium binding ability of high G residue containing alginates, thus the ion exchange process between the wound exudates and the alginate bandage is slow, whereas in high M residue containing alginates the calcium ions are replaced by sodium ions more readily which contributes to their increased swelling capacity (Gopalakrishnan, 2006). This difference can be explained by the internal arrangement of the G: M residues with fewer homopolymeric, consecutive GGGG or MMMM blocks and more alternating GMGM motifs present in the alginates tested. Taken together, $CaSO_4$ pre-crosslinking does not affect the hydration or swelling properties of alginate bio-inks tested.

The Effect of Alginate Molecular Weight, G: M Ratio and Pre-crosslinking on the Diameter of Wet Spun Alginate Fibers

To determine whether CaSO4 pre-crosslinking affects the diameter of the wet spun alginate fibers, the fibers (controls and pre-crosslinked) were prepared, photographed, the diameters were measured using the Cytation Image Analysis software and compared. Overall, alginates with the lowest molecular weight and very low viscosity (VLVG, VLVM) produced fibres with the largest diameter, irrespective of pre-crosslinking. This could be explained by lower molecular weight of these low viscosity alginates, as fewer crosslinking sites are available to entrap calcium ions in the polymer chains. The diameters of LVG and LVM alginates of low viscosity were in the middle and high molecular weight alginates (MVG and MVM) produced fibres with the smallest diameter. No significant differences were observed between control and pre-crosslinked alginate fibres of the same alginate type (e.g. VLVG control and VLVG pre-crosslinked), yet significant differences between alginate types were observed. VLVG control was significantly different (<0.0001) to: LVG control and pre-crosslinked alginate, MVG control and pre-crosslinked alginate, VLVM control and pre-crosslinked alginate, LVM control and pre-crosslinked alginate, and MVM control and pre-crosslinked alginate. Pre-crosslinked VLVG exhibited the exact same differences with other alginate types as VLVG control. LVG control was significantly different (<0.0001) to VLVM control and pre-crosslinked alginate, LVM control and pre-crosslinked alginate, MVM control and pre-crosslinked alginate. Pre-crosslinked LVG exhibited the exact same significant differences to other alginate types as LVG

control. The diameters of LVG control alginate and LVG pre-crosslinked alginate were not significantly different to MVG control alginate or pre-crosslinked MVG alginate. Similarly, no significant differences were observed between control and pre-crosslinked LVM and MVM alginates. Results are presented in **Figure 2Ai** shows the images of control alginate fibers, (**Figure 2Aii**) shows the pre-crosslinked alginate fibers and comparison of diameters of control and pre-crosslinked alginate fibers is presented in (**Figure 2Aiii**).

G:M ratio is known to be an important modulator of the physiochemical properties of alginate gels. It has been proposed that only G residues are involved in the intermolecular crosslinking of the polymer chains with divalent cations to produce hydrogels. Crosslinking can be accomplished when guluronic residues bend and encounter the divalent cation creating an "egg-box" structure whereby the sodium ions of the G blocks are substituted by the calcium ions. Alginates with a high prevalence of G block units are known to possess higher porosity, rigidity, mechanical stability and are more brittle. The higher porosity of G alginates due to the conformation of the G blocks can explain why they produce fibers with larger diameters compared to M alginates. On the contrary, alginates with a high proportion of M blocks are more elastic and less porous (Singh et al., 2010; Fu et al., 2011; Giri et al., 2012; Abasalizadeh et al., 2020). Another explanation for the observed change in diameter between the different alginates could be due to the stereochemical arrangement of the uronic acid unit conformation, as MM blocks have been shown to be di-equatorially linked at C-1 and C-4, creating a flat, ribbon-like, straight polymer chain, while the GG block is formed from diaxial groups at both C-1 and C-4, forming a bucked polymer chain. X ray studies propose that alginates with a higher M content have smaller spacings (10.35 Å) along the polysaccharide chain axis compared to alginates with a greater G content (8.72 Å). These variations in composition affect the physiochemical properties of alginate. (Penman and Sanderson, 1972; Atkins et al., 1973; Qin, 2008). Whilst a difference in diameter between the control and pre-crosslinked alginate fibers was expected due to the increased intermolecular binding of the polymer chains in pre-crosslinked alginates, no significant differences were observed. A possible explanation for this could be the very low concentration of calcium ions in the pre-crosslinker used (0.001 M $CaSO_4$) compared to the much greater concentration of available calcium ions in the crosslinking bath (0.1 M $CaCl_2$). Alginates are likely to be saturated with calcium ions when deposited in the post-crosslinking bath minimizing any effect of the low concentration of calcium ions in the pre-crosslinking solution. Taken together, pre-crosslinked alginate fibers can be extruded at a given diameter/resolution with no shrinkage of post-print resulting in high predictability and consistency of the final construct.

Effect of $CaSO_4$ Pre-crosslinking on Alginate-Based Bio-Ink Viscosity

The aim of this study was to improve printability of low concentration alginate-based bio-inks to increase the viscosity. These experiments aimed to assess the difference in change of viscosity between control alginates and pre-crosslinked alginates. Viscosity was assessed over a range of shear rates 0–10 y(s-1). It is evident that viscosity of pre-crosslinked alginates significantly increases compared to the controls in all alginates tested. This increase in viscosity is particularly evident in MVM alginate, followed by MVG alginate and LVM alginate, compared to all the other pre-crosslinked alginates tested and non-pre-crosslinked controls. As the shear rate increases the viscosity of all alginates tested decreases, which suggests that all alginate controls and pre-crosslinked gels exhibit shear thinning (also called pseudoplastic flow) behaviour characteristic of non-Newtonian fluids. At critical shear rate a large drop of viscosity is observed in pre-crosslinked alginates, this drop signifies the start of shear thinning region. The shear thinning index was calculated and a significant difference can be observed between the control and pre-crosslinked alginate bio-inks. This relationship is evident in all alginates tested. Results are presented in **Figure 3Ai** shows the viscosity of control alginates tested, (**Figure 3Aii**) shows the change in viscosity of the pre-crosslinked alginates. These results are in agreement with Gonzalez-Fernandez et al., 2021 and Freeman and Kelly, 2017 and who also observed an increase in viscosity and printability in their studies where alginate bio-inks were crosslinked with $CaSO_4$, albeit at much higher alginate concentrations. The authors report that their results demonstrated that the Mw of alginate bio-inks had a significant effect viscosity and subsequent printability (Freeman and Kelly 2017; Gonzalez-Fernandez et al., 2021). To calculate the shear thinning index a ratio was obtained by dividing apparent viscosity at the lowest speed by the apparent viscosity at the highest speed (Wypych, 2017). Alginates with a higher molecular weight, particularly MVG and MVM, exhibit the most shear thinning in the pre-crosslinked state, indicating their improved suitability to be used as bio-inks in 3D bio-printing. These results are presented in **Figure 3B**.

It can be observed that the overall trends in terms of viscosity remain similar when considering the Mw of different alginates before and after pre-crosslinking. Although MVM and MVG alginate controls are remarkably similar in terms of Mw and viscosity, there is an increase in viscosity of 10 Pas in the pre-crosslinked MVM alginate (41.9 Pas) compared to MVG alginate (30.1 Pas). Additionally, it can be observed that high-M containing alginates experience a greater change in viscosity compared to high-G containing alginates. Mw affects viscosity, as alginates with a higher Mw (MVM and MVG) have the highest viscosity post pre-crosslinking with $CaSO_4$. However, frequency of G residues in alginate polymers does not seem to be a determining factor for the observed change in viscosity. This is particularly evident in the VLVG alginate, which has a frequency of G residues of 70, yet exhibits very low viscosity in both the control (0.01 Pas) and the pre-crosslinked state (0.408 Pas). It is interesting to observe the difference between VLVM alginate and MVM alginate. In the control both of those alginates have the same relative frequency of G residues and exhibit the same viscosity, however, after pre-crosslinking the viscosity of VLVM alginate increases to 14.89 Pas, yet pre-crosslinked MVM alginate (40.41 Pas) exhibits a 100-fold increase of

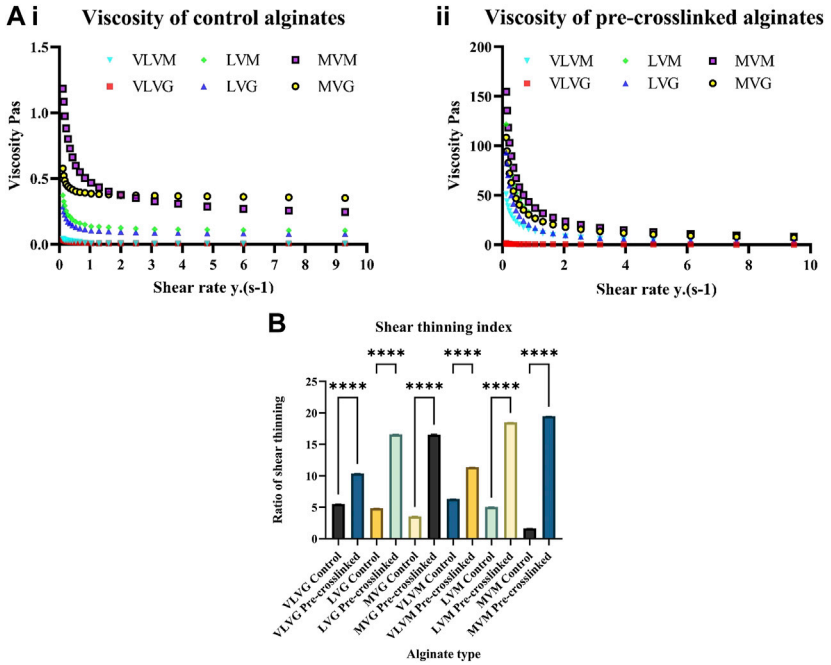

FIGURE 3 | Effect of $CaSO_4$ pre-crosslinking on alginate-based bio-ink viscosity. Assessment of viscosity of control **(Ai)** and pre-crosslinked **(Aii)** alginate bio-inks was performed using a rotational rheometer. Shear thinning index was calculated by dividing apparent viscosity at the lowest speed by the apparent viscosity at the highest speed **(B)**. Values are expressed as mean ± SD from six separate experiments with asterisks representing significance from control values (****, $p < 0.0001$).

viscosity compared to the non-pre-crosslinked state (0.404 Pas). This observed behavior confirms that a high molecular weight alginate with a high M frequency will show the greatest degree of increase in viscosity after pre-crosslinking with $CaSO_4$.

Shear Rheological Assessment

Shear rate ramps were performed to analyze the flow behavior of tested alginate-based bio-inks. An oscillation frequency sweep was conducted at 25°C over a frequency range of 0.1–10 Hz from which rheological data was collected. All data was performed on 6 independent samples for all the alginates tested, control alginates and alginates pre-crosslinked with $CaSO_4$. The storage moduli of control and pre-crosslinked alginates are presented in **Figures 4Ai,ii**, the loss moduli are presented in (**Figures 4Bi,ii**) and the phase angles of the control and pre-crosslinked alginates are presented in (**Figures 4Ci,ii**). Briefly, the elastic component of the viscoelastic sample is characterized by the storage modulus (G′), which describes the solid-like behavior of the sample. The viscous component of the sample is characterized by the loss modulus (G″), which refers to the liquid-like behavior of the sample. In viscoelastic solids G' > G″, due to the chemical bonds and physio-chemical interactions inside the material. In viscoelastic liquids G" > G′, due to the absence of strong bonds between the individual molecules in the material. The phase angle (tan, δ) is a factor that depicts the ratio of the elastic behavior to viscous behavior in a viscoelastic sample. The phase angle is always between 0° and 90°. This is because for ideally elastic (solid) behavior there is no viscous component (G" = 0). Ideally viscous behavior (liquid) is represented by $\delta = 90°$, this is because G' = 0, meaning there is no elastic component present in this sample. The phase angle can indicate the phase transition (sol-gel transition point) of the sample that happens during measurement (Anton paar, 2010, Gonzalez-Fernandez et al., 2021).

The obtained values of the storage and loss moduli in both VLVG control and pre-crosslinked VLVG are very low at all frequencies tested (G′ between 0 and 4 Pa in both alginates, G″ between 0 and 4 Pa) in both alginates. This behaviour is characteristic of a liquid, which is further confirmed by the phase angle of 90° in VLVG control and 80° in pre-crosslinked VLVG. Although pre-crosslinking does decrease the phase angle from 90 to 80°, at the concentrations tested the effect is not strong enough to produce a gel at this concentration of alginate and pre-crosslinker. Similar low storage and loss modulus values were found in LVG control, indicating that the material exhibits the behavior of a liquid. The phase angle ranges between 70 and 80°, thus liquid like behaviour of the material predominates. In the pre-crosslinked LVG alginate the storage modulus (values range from 90 to 120 Pa) exceeds the loss modulus (values range from 2 to 26 Pa) at all frequencies tested indicating a shift towards solid-like behaviour of the material due to pre-crosslinking. The phase angle values range between 10 and 16° throughout the range of shear frequencies. This behaviour indicates that a strong solid-like component predominates in the material due to the pre-crosslinking effect, forming a gel. In MVG control, again very low values of the storage and loss moduli can be observed. The phase angle ranges from 62 to 70° indicating the behaviour of a weak viscoelastic liquid. Yet, with increase in molecular weight of

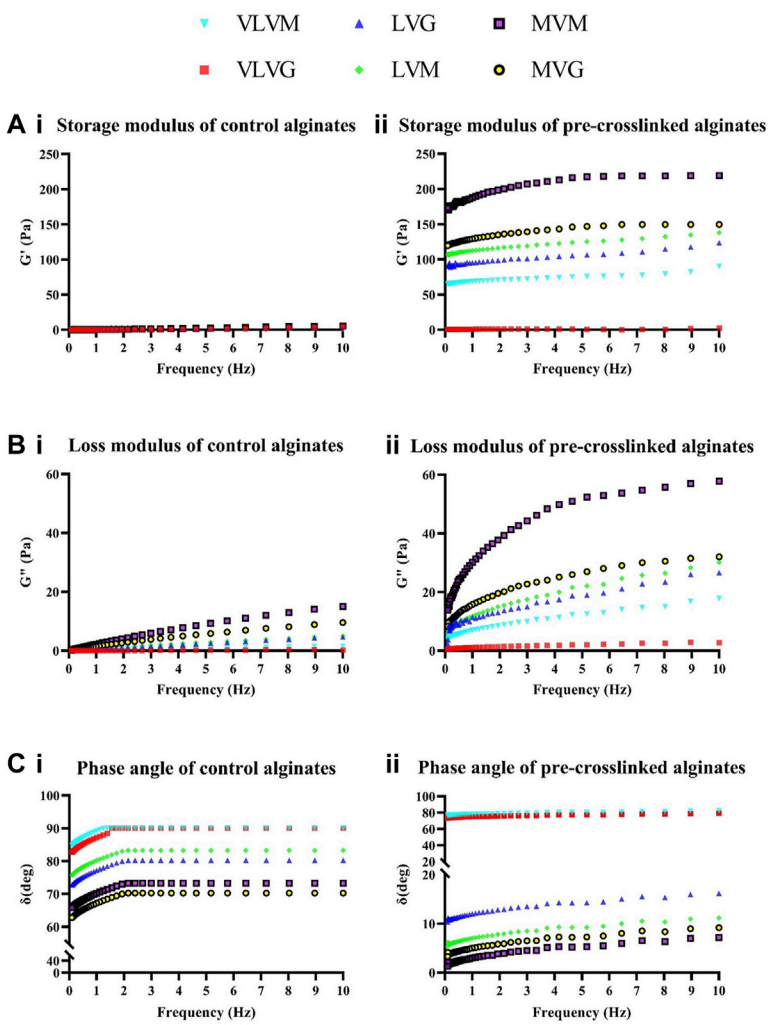

FIGURE 4 | Shear rheological assessment. Assessment of rheological parameters of control and pre-crosslinked alginate bio-inks was performed using a rotational rheometer. Storage moduli of control **(Ai)** and pre-crosslinked **(Aii)** alginates, loss moduli of control **(Bi)** and pre-crosslinked **(Bii)** alginates and phase angle of control **(Ci)** and pre-crosslinked **(Cii)** alginates were measured. Values are expressed as means from six separate experiments.

alginates, the phase angle values in control alginates increase and a stronger material is produced when comparing to VLVG and LVG alginate. The phase angle does not reach 90° as is the case with VLVG alginate, thus indicating that at shear rates tested the material does not adopt a complete liquid-like behaviour. In the pre-crosslinked MVG alginate a strong solid-like behaviour can be observed when looking at G' (values range between 119 and 149.5 Pa) exceeding G" (values range between 8 and 32 Pa) at all frequencies tested, which is further confirmed by the phase angle value of 10° at shear rate 10 Hz. The trends between control VLVM alginate and pre-crosslinked VLVM alginate are very similar to VLVG control and pre-crosslinked VLVG. In VLVM control the loss modulus exceeds the storage modulus at all frequencies indicating that the material behaves like a liquid. The phase angle ranges from 84 to 90° further confirming that. The effect of pre-crosslinking minimally influences gel strength in VLVM alginate, as the loss modulus still exceeds the storage modulus and phase angle ranges from 76 to 82°. LVM control exhibits low storage and loss modulus values, as expected with the phase angle ranging from 75 to 83°, indicating liquid like behaviour of the sample. In pre-crosslinked LVM the storage modulus exceeds the loss modulus significantly at all frequencies tested. Storage modulus values range from 106 to 138 Pa and loss modulus values range from 6 to 30 Pa, indicating that pre-crosslinking significantly affected the physiochemical properties of the produced gel. This is further confirmed by the phase angle value of 11 at 10 Hz. The most significant change in physiochemical parameters is observed in MVM alginate, where MVM control exhibits the behaviour of a viscoelastic liquid with storage and loss values being very low and loss modulus exceeding the storage modulus at all frequencies tested, as with all the control alginates tested. However, in pre-crosslinked MVM the storage modulus ranges from 172 to 219 Pa and the loss modulus ranges from 13 to 57 Pa, indicating a

transition from a liquid-like behaviour to a strong gel. Interestingly, the difference between the values of MVM control and pre-crosslinked MVM is the greatest observed among all the alginates tested. This can be explained by the higher Mw of the alginate, yet MVG alginate is very similar in terms of Mw to MVM alginate and did not produce such a drastic response to pre-crosslinking. Perhaps his effect can be explained by unsaturated crosslinking density, whereby in G rich alginates more free valences are available for crosslinking to occur, yet the concentration of CaSO4 is so low that not all the available sites are engaged. An inverse relationship could take place in high M alginates where fewer valences are available and a higher degree of saturation with the calcium ions takes place. This diminished saturation due to low concentration of calcium ions could be a potential explanation to why the effect of pre-crosslinking is realised to a lesser degree in high G containing alginates.

Overall, in control alginates viscous properties exhibit an overall dominance over elastic properties. Pre-crosslinked alginates exhibit stronger elastic properties that are indicative of firmer gels, when compared to pure alginate controls, due to the increase in interconnecting networks between the polymer structures as a result of pre-crosslinking. The increase in shear-thinning behavior of the pre-crosslinked alginate bio-inks implies a robust interaction between polysaccharide molecules and the crosslinking ions, which leads to a greater degree of entanglement between the microstructures and is responsible for better shape fidelity observed post printing. These results are in line with previously described study by Jessop et al., who have investigated the shear rheological parameters of alginate bio-inks with the addition of nanocellulose (Jessop et al., 2019). Kim et al., 2019 have also assessed rheological parameters of alginate pre-crosslinked with $CaSO_4$ albeit at considerably higher concentrations of alginate (2%) and $CaSO_4$ (1%). The results of this study confirmed increase of the storage modulus over the loss modulus in the pre-crosslinked state as well as lower storage modulus compared to loss modulus in the 0% $CaSO_4$ alginate control (Kim et al., 2019). Improved phase angle accompanied with maintenance of shear thinning properties is anticipated to improve printability (Gao et al., 2018).

Effect of Pre-crosslinking on Bio-Ink Printability

Mechanical properties of alginate bio-inks, such as Mw and stiffness can influence cell-matrix interaction and behavior such as adhesion and differentiation. Thus spatial alteration of the stiffness of bio-inks and modulating the rigidity of the final 3D bio-printed construct can not only improve the final print resolution but can be used to direct cell fate and growth characteristics of the encapsulated cells (Freeman and Kelly, 2017; Gonzalez-Fernandez et al., 2021). Concomitantly, too high viscosity and crosslinking density result in reduced pore size leading to compromised mass transfer of waste and nutrients and subsequent decline in cell viability (Reddy and Pandit, 2016). A golden bio-fabrication window for rational design of bio-inks requires compromise between printability and biocompatibility (Chimene et al., 2016). To further improve the design of 3D bio-printed constructs and achieve high resolution printing of microstructures, quantitative models can be used to take the responses of programmed human or bacterial cells into consideration. This in turn allows for the development of novel living devices enabled by the 3D printing of manipulated cells such as logic gates, spatiotemporally responsive patterning, and wearable devices as demonstrated by Liu et al., 2018. Genetic engineering of living cells to possess a variety of functions such as chemical secretion, drug production, bio-sensing and apoptosis is possible and can be programmed by accounting for the microstructure of the hydrogel matrices and the distribution of cells and chemicals within those matrices. This allows for simulation of substance diffusion and cellular activity in the bio-printed construct under a range of conditions, thus providing more feedback and guidance for design of living materials and devices with predictable responses (Liu et al., 2018).

To assess the printability of the bio-inks, control alginates and pre-crosslinked bio-inks were bio-printed at a steady rate of extrusion at 45–65 kPa in a shape of a lattice and photographed. Results and a schematic representation of the process are presented in **Figures 5Ai–iii,B**. Due to the low concentration of alginate used (1.2%), it was expected to see minimal print resolution, particularly in the control alginates, as was the case. Based on the viscometrical and rheological assessment it was expected that pre-crosslinked MVG, MVM, LVM or LVG bio-inks would produce a construct with the most desirable printability characteristics, due to the similarity in their viscosities in the pre-crosslinked state. However, during the bio-printing process it has become apparent that pre-crosslinked MVG alginate was not suitable for the bio-printing process due to hydrocolloid formation in the printing needle preventing successful extrusion in a lattice shape at the extrusion pressures tested. LVG alginate lattice did not maintain the resolution of the structure, the shape fidelity has been compromised and no distinguishable gaps between the bio-printed lines were observed, the lines have merged into a single square. A similar problem was observed when looking at the print produced using the pre-crosslinked LVM alginate bio-ink, limited gaps between the lines were present. Pre-crosslinked MVM alginate produced the best bio-printed lattice with clear gaps between the bio-printed lines throughout the structure and thus was selected for subsequent experiments elucidating CSF viability in these inks. To include a positive control, CELLINK, commercially available bio-ink, was purchased, and a lattice was bio-printed using the same extrusion pressure and needle. The needle used is displayed in **Figure 5C**. **Figure 5D** shows the top view of the bio-printed lattice obtained by extruding pre-crosslinked MVM alginate, the side view of the 4 layered lattice is displayed in **Figure 5F**. **Figure 5E** shows the top view of the positive control—lattice bio-printed with CELLINK bio-ink. The line diameter of structures produced with CELLINK and pre-crosslinked MVM alginate was measured using the BioTek Gen5 data analysis software and compared with the line diameter of pre-crosslinked MVM alginate. This data is presented in **Figure 5G**. No significant differences in line diameter from pre-crosslinked MVM alginate lattice and

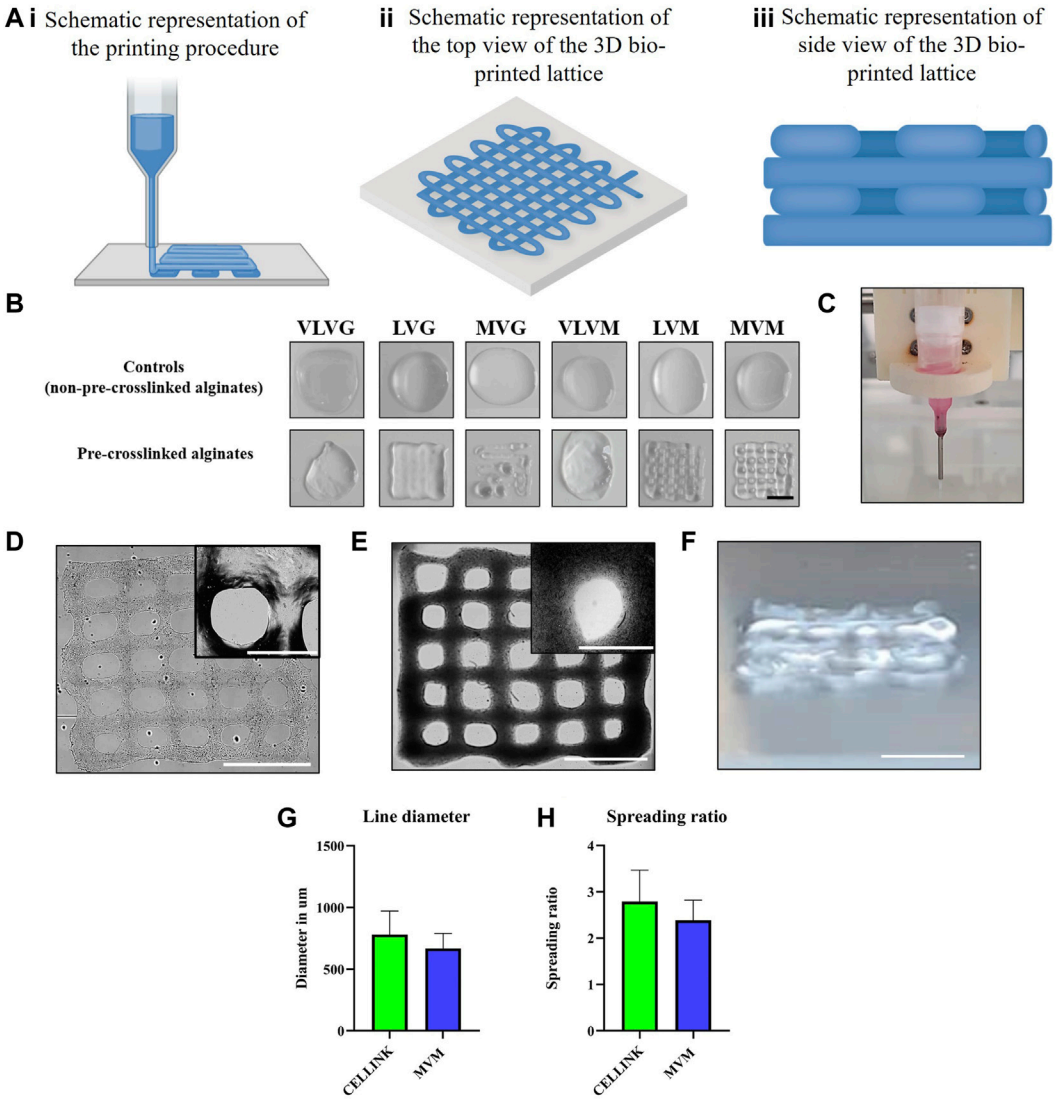

FIGURE 5 | Effect of pre-crosslinking on bio-ink printability. Schematic design of the 3D bio-printed lattices is illustrated in **(Ai–Aiii)** with schematic representation of the printing procedure being presented in **(Ai)**, schematic representation of the top view of the bio-printed lattice presented in **(Aii)** and the side view of the bio-printed lattice consisting of 4 layers is schematically represented in **(Aiii)**. Low viscosity alginates were 3D bio-printed in a shape of a lattice and imaged **(B)**. 30G PTFE lined needle was used during the bio-printing process **(C)**. Bio-printed pre-crosslinked MVM alginate lattice at 10x magnification and 40x magnification, scalebars represent 1000 µm and 3,000 µm respectively. **(D)**, bio-printed CELLINK positive control lattice at 10x magnification and 40x magnification, scalebars represent 1000 µm and 3000 µm respectively **(E)**. Photograph of the side view of the bio-printed lattice is displayed in **(F)**, scalebar represent 1000 µm. Line diameters were calculated from **(D)** and **(E)** and are displayed in **(G)**. Spreading ratio was calculated by dividing line diameter by the internal needle diameter (280 µm) **(H)**.

CELLINK lattice were observed, suggesting that pre-crosslinked MVM is suitable for use as a bio-ink. Based on this data, the swelling ratio was calculated using the formula Swelling ratio = Printed fiber diameter/Inner needle diameter (inner diameter of the needle in this study was 280 µm). These results are presented in **Figure 5H**. No significant differences between CELLINK bio-ink and pre-crosslinked MVM alginate bio-ink in terms spreading were observed. Overall, it has been demonstrated that pre-crosslinked MVM alginate bio-ink was able to produce a layered lattice (4 layers) with significant improvement in shape fidelity as compared to the non-pre-crosslinked alginate controls.

Evaluation of CSF Viability in Pre-crosslinked Bio-Inks

Viability of CSFs was assessed in both the wet spun fibers (**Figure 6**) as well as the bio-printed constructs (**Figure 7**) using a metabolic assay—CellTiterGlo and confirmed by Calcein AM/Ethidium Homodimer 1 (CAM/EthD-1) live/dead

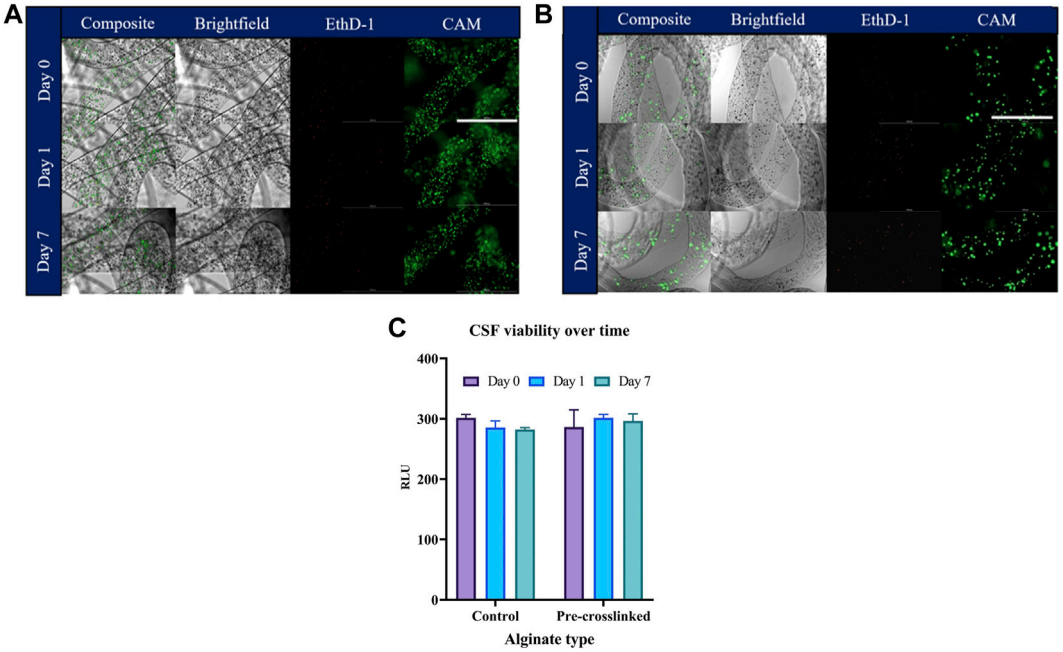

FIGURE 6 | Evaluation of CSF viability in pre-crosslinked alginate fibers. Cell-laden fibers were formed by wet spinning prior to being stained with CAM (live stain) and Ethd-1 (dead stain) and imaged. Control alginate fibers are presented in **(A)**, pre-crosslinked alginate fibers are presented in **(B)**, metabolic assessment of CSF viability by CellTiterGlo is displayed in **(C)**. Values are expressed as mean ± SD from three separate experiments. Scalebar corresponds to 1000 μm.

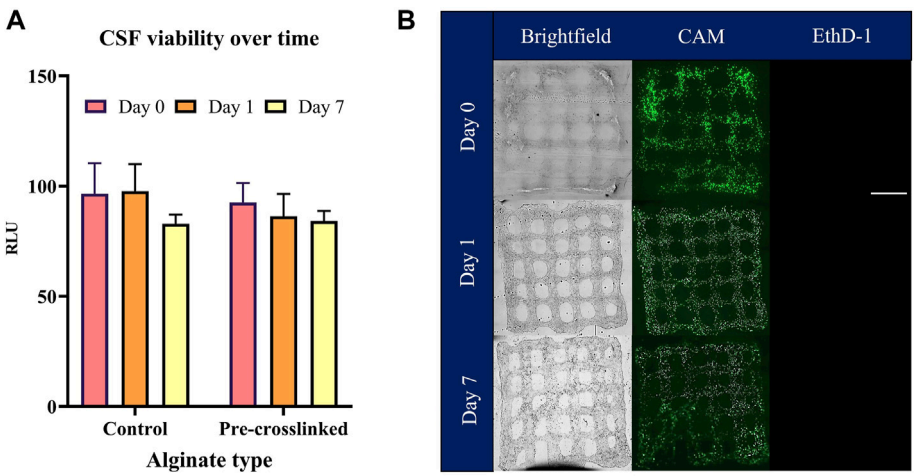

FIGURE 7 | Evaluation of CSF viability in pre-crosslinked alginate bio-inks. Cell-laden bio-inks were bio-printed prior to being assessed for metabolic activity (CSF viability) by CellTiterGlo. CELLINK bio-ink was used as a positive control **(A)**. Encapsulated cells were assessed for viability with CAM (live stain) and Ethd-1 (dead stain) and imaged **(B)**. Values are expressed as mean ± SD from three separate experiments.

fluorescent staining. **Figure 6A** illustrates live/dead staining performed on CSFs encapsulated in control alginate fibers, (**Figure 6B**) shows the CSFs in pre-crosslinked alginate fibers immediately after wet spinning (day 0), after 1 day in culture and after a week in culture. Cell viability and metabolic assessment was performed in both the wet spun alginate fibers as well as the bio-printed constructs to be able to differentiate the potential cell detrimental effect that can take place during the bio-printing procedure. The post-crosslinking time in the wet spun fibers was 10 min, however, bio-printed constructs were post-crosslinked for 2 min, due to the small size of the lattice, to reduce the crosslinking time that the construct is exposed to. No significant differences in CSF viability as assessed by CellTiterGlo between the control (non-pre-crosslinked) alginate-based bio-inks and the

pre-crosslinked MVM alginate were observed over the culture period of 7 days in wet spun alginate fibers (**Figure 6C**). These results are confirmed by the live/dead staining, where live cells can be seen in pre-crosslinked alginate fibers and in control MVM alginate fibers. Similar trends in terms of cell viability can be observed in **Figure 7A** where CellTiterGlo assay was performed on CSFs bio-printed with CELLINK (positive control) and pre-crosslinked MVM alginate (pre-crosslinked). Results of live/dead staining preformed on pre-crosslinked MVM alginate lattices are presented in **Figure 7B** where live cells can be seen at all time points tested.

The bio-printing procedure can influence final cell viability. Various factors can affect cell viability and need to be considered, such as the shear stress that cells experience during the extrusion process, needle diameter, gelation conditions, post-crosslinking time and concentration of the crosslinker used as well as fabrication time. In this study by using a low concentration of pre-crosslinker to modify the viscosity of low percentage alginate bio-inks greater shear thinning index of the inks was achieved and the effect of shear stress was minimized. It has been shown that the use of calcium sulfate promotes internal gelation whereby the calcium is released gradually and in a controlled manner simultaneously through the whole system, which creates a more homogenous, less dense network compared to gelation achieved by the more rapid diffusion process (Mancini and McHugh, 2000; Choi et al., 2002; Lee and Rogers, 2012). Gonzalez-Fernandez et al., 2021 have found that alginate pre-crosslinked with $CaSO_4$ can be bio-printed at lower extrusion pressures compared to alginate pre-crosslinked with the equivalent concentration of $CaCl_2$ due to the lower solubility of sulfate salts and slower dissociation rate of calcium ions which promote gradual, more controlled gelation kinetics (Gwon et al., 2015). The authors suggest that this uncontrolled gelation with $CaCl_2$ can have a detrimental effect on the final printability of the bio-ink when compared to more homogenous alginate bio-inks pre-crosslinked with $CaSO_4$ or calcium carbonate ($CaCO_3$). It has also been reported by Freeman et al., that extrusion of bio-inks pre-crosslinked with $CaCl_2$ required higher pressures to print the inks compared to bio-inks pre-crosslinked with $CaSO_4$, which again can have a detrimental effect on the cell viability after the extrusion process (Freeman and Kelly, 2017). In this study, no detrimental effects to CSFs immediately after bio-printing and over the culture period have been observed, potentially due to the shear thinning properties of the bio-inks, low concentration of alginate used to facilitate effective mass transfer of nutrients and waste in culture and reduced post-crosslinking time. Additionally, the use of a PTFE lined needle has been shown to reduce the shear stress the cells experience by reducing friction and adhesion of the biomaterial to the needle. PTFE is a synthetic fluoropolymer that possess desirable properties such as low friction coefficient and hydrophobicity, both help to reduce shear stress that cells experience during the extrusion process (Foust, 2014).

It has been previously demonstrated that alginate sulfate gels are non-toxic to chondrocytes in 1% alginate and good cell viability, proliferation and collagen II synthesis was observed by the encapsulated cells (Müller et al., 2017). However, Gonzalez-Fernandez et al., have described that the change in physical properties in alginate-$CaSO_4$ pre-crosslinked bio-inks has affected the biological performance of the encapsulated mesenchymal stem cells. The authors report high cell apoptosis in the bio-printed constructs 7 days after printing. These effects were not observed in the current study, perhaps due to the lower percentage of alginate (1.2% instead of 3.5%) and $CaSO_4$ (0.001 M instead of 50 mM) used. Another possible explanation of the observed differences could be the addition of RGD motifs into the alginate $CaSO_4$ bio-inks described by Gonzalez-Fernandez et al. RGD motifs are a site for integrin binding, which could result in a higher cell sensitivity to rigid or non-compliant matrices. Pre-crosslinked alginate bio-inks at 3% could reduce this mechano-sensing in the bio-printed construct which could potentially explain the reduced viability of cells over time (Gonzalez-Fernandez et al., 2021).

CONCLUSION

The overall aim of this study was to improve printability of low concentration alginate bio-inks without compromising the biocompatibility of the final printed structure. To accomplish this the viscosity of low concentration alginates was increased by pre-crosslinking with a low concentration of calcium sulfate, which increased the viscosity and made alginate suitable for the bio-printing process at the lowest printable alginate concentration. It is well established that higher alginate concentrations can facilitate printability of extrusion-based bio-inks, yet this can be detrimental to cell viability. Here we demonstrate a simple and cost-effective method whereby cell viability can be supported in culture using low concentrations of alginate without compromising print fidelity or post-print material properties.

DATA AVAILABILITY STATEMENT

The raw data supporting the conclusion of this article will be made available by the authors, without undue reservation.

AUTHOR CONTRIBUTIONS

AK: conception and design, collection and/or assembly of data, data analysis and interpretation, manuscript writing, final approval of manuscript. SS: data analysis and interpretation, manuscript writing, final approval of manuscript. CC: conception and design, final approval of manuscript.

SUPPLEMENTARY MATERIAL

The Supplementary Material for this article can be found online at: https://www.frontiersin.org/articles/10.3389/fmech.2022.867685/full#supplementary-material

Supplementary Figure S1 | The effect of alginate molecular weight, G:M ratio and pre-crosslinking on the swelling properties of bio-inks. Fibers were formed by wet spinning before assessing wet weight and dry weight of control and pre-crosslinked alginate fibers. Weight values were used to calculate swelling % of control alginate

fibers [ai] and pre-crosslinked alginate fibers [aii]. Values are expressed as mean ± SD from six separate experiments.

Supplementary Figure S2 | Video of the 3D bio-printing process of the lattice. This video was taken to further illustrate the 3D bio-printing process to produce a lattice using CaSO4 pre-crosslinked MVM alginate bio-ink.

Supplementary Figure S3 | Illustration and video of the 3D bio-printing process producing an acellular ring. An acellular ring (6 layers) with the $CaSO_4$ pre-crosslinked MVM alginate without subsequent $CaCl_2$ post-crosslinking was 3D bio-printed for demonstrative purposes that our bio-ink can retain its structure as a free-standing filament, photograph and video of the printing process are available.

REFERENCES

Abasalizadeh, F., Moghaddam, S. V., Alizadeh, E., akbari, E., Kashani, E., Fazljou, S. M. B., et al. (2020). Alginate-based Hydrogels as Drug Delivery Vehicles in Cancer Treatment and Their Applications in Wound Dressing and 3D Bioprinting. *J. Biol. Eng.* 14 (1), 8. doi:10.1186/s13036-020-0227-7

Ahn, S., Lee, H., Puetzer, J., Bonassar, L. J., and Kim, G. (2012). Fabrication of Cell-Laden Three-Dimensional Alginate-Scaffolds with an Aerosol Cross-Linking Process. *J. Mater. Chem.* 22 (36), 18735–18740. doi:10.1039/C2JM33749E

Anton Paar (2010). *Basics of rheology: Anton Paar Wiki*. Available at: https://wiki.anton-paar.com/uk-en/basics-of-rheology/ (Accessed August 11, 2020)

Atkins, E. D. T., Nieduszynski, I. A., Mackie, W., Parker, K. D., and Smolko, E. E. (1973). Structural Components of Alginic Acid. I. The Crystalline Structure of Poly-?-D-Mannuronic Acid. Results of X-ray Diffraction and Polarized Infrared Studies. *Biopolymers* 12 (8), 1865–1878. doi:10.1002/bip.1973.360120813

Bishop, E. S., Mostafa, S., Pakvasa, M., Luu, H. H., Lee, M. J., Wolf, J. M., et al. (2017). 3-D Bioprinting Technologies in Tissue Engineering and Regenerative Medicine: Current and Future Trends. *Genes Dis.* 4 (4), 185–195. doi:10.1016/j.gendis.2017.10.002

Braccini, I., and Pérez, S. (2001). Molecular Basis of Ca2+-Induced Gelation in Alginates and Pectins: The Egg-Box Model Revisited. *Biomacromolecules* 2 (4), 1089–1096. doi:10.1021/bm010008g

Chen, C.-G., Gerelt, B., Jiang, S.-T., Nishiumi, T., and Suzuki, A. (2006). Effects of High Pressure on pH, Water-Binding Capacity and Textural Properties of Pork Muscle Gels Containing Various Levels of Sodium Alginate. *Asian Australas. J. Anim. Sci.* 19 (11), 1658–1664. doi:10.5713/ajas.2006.1658

Chimene, D., Lennox, K. K., Kaunas, R. R., and Gaharwar, A. K. (2016). Advanced Bioinks for 3D Printing: A Materials Science Perspective. *Ann. Biomed. Eng.* 44 (6), 2090–2102. doi:10.1007/s10439-016-1638-y

Choi, B. Y., Park, H. J., Hwang, S. J., and Park, J. B. (2002). Preparation of Alginate Beads for Floating Drug Delivery System: Effects of CO(2) Gas-Forming Agents. *Int. J. Pharm.* 239 (1), 81–91. doi:10.1016/S0378-5173(02)00054-6

Chung, J. H. Y., Naficy, S., Yue, Z., Kapsa, R., Quigley, A., Moulton, S. E., et al. (2013). Bio-ink Properties and Printability for Extrusion Printing Living Cells. *Biomater. Sci.* 1 (7), 763–773. doi:10.1039/C3BM00012E

Ck, K., and Px, M. (2001). Ionically Crosslinked Alginate Hydrogels as Scaffolds for Tissue Engineering: Part 1. Structure, Gelation Rate and Mechanical Properties. *Biomaterials* 22 (6), 511. doi:10.1016/s0142-9612(00)00201-5

Donderwinkel, I., van Hest, J. C. M., and Cameron, N. R. (2017). Bio-inks for 3D Bioprinting: Recent Advances and Future Prospects. *Polym. Chem.* 8 (31), 4451–4471. doi:10.1039/C7PY00826K

Draget, K. I., Skjåk-Bræk, G., and Stokke, B. T. (2006). Similarities and Differences between Alginic Acid Gels and Ionically Crosslinked Alginate Gels. *Food Hydrocolloids* 20, 170–175. doi:10.1016/J.FOODHYD.2004.03.009

Elkayam, T., Amitay-Shaprut, S., Dvir-Ginzberg, M., Harel, T., and Cohen, S. (2006). Enhancing the Drug Metabolism Activities of C3A- A Human Hepatocyte Cell Line-By Tissue Engineering within Alginate Scaffolds. *Tissue Eng.* 12 (5), 1357–1368. doi:10.1089/ten.2006.12.1357

Fedorovich, N. E., Schuurman, W., Wijnberg, H. M., Prins, H.-J., van Weeren, P. R., Malda, J., et al. (2012). Biofabrication of Osteochondral Tissue Equivalents by Printing Topologically Defined, Cell-Laden Hydrogel Scaffolds. *Tissue Eng. C: Methods* 18 (1), 33–44. doi:10.1089/ten.TEC.2011.0060

Fontes, A. B., and Marcomini, R. F. (2020). 3D Bioprinting: a Review of Materials, Processes and Bioink Properties. *jCEC* 6, 0617–0639. doi:10.18540/jcecvl6iss5pp0617-0639

Foust, S. A. (2014). *Ultrathin PTFE Coating for Hypodermic Needles Enabled by Mussel-Inspired PDA Adhesive Layer*. Fayetteville: University of Arkansas, ScholarWorks, 40.

Freeman, F. E., and Kelly, D. J. (2017). Tuning Alginate Bioink Stiffness and Composition for Controlled Growth Factor Delivery and to Spatially Direct MSC Fate within Bioprinted Tissues. *Sci. Rep.* 7 (1), 17042. doi:10.1038/s41598-017-17286-1

Fu, S., Thacker, A., Sperger, D. M., Boni, R. L., Buckner, I. S., Velankar, S., et al. (2011). Relevance of Rheological Properties of Sodium Alginate in Solution to Calcium Alginate Gel Properties. *AAPS PharmSciTech* 12 (2), 453–460. doi:10.1208/s12249-011-9587-0

Gao, T., Gillispie, G. J., Copus, J. S., Pr, A. K., Seol, Y.-J., Atala, A., et al. (2018). Optimization of Gelatin-Alginate Composite Bioink Printability Using Rheological Parameters: a Systematic Approach. *Biofabrication* 10 (3), 034106. doi:10.1088/1758-5090/aacdc7

Gasperini, L., Maniglio, D., Motta, A., and Migliaresi, C. (2015). An Electrohydrodynamic Bioprinter for Alginate Hydrogels Containing Living Cells. *Tissue Eng. Part C: Methods* 21 (2), 123–132. doi:10.1089/ten.TEC.2014.0149

Gillispie, G., Prim, P., Copus, J., Fisher, J., Mikos, A. G., Yoo, J. J., et al. (2020). Assessment Methodologies for Extrusion-Based Bioink Printability. *Biofabrication* 12 (2), 022003. doi:10.1088/1758-5090/ab6f0d

Giri, T. K., Thakur, D., Alexander, A., Ajazuddin, Badwaik, H., and Tripathi, D. K. (2012). Alginate Based Hydrogel as a Potential Biopolymeric Carrier for Drug Delivery and Cell Delivery Systems: Present Status and Applications. *Cdd* 9 (6), 539–555. doi:10.2174/156720112803529800

Gonzalez-Fernandez, T., Tenorio, A. J., Campbell, K. T., Silva, E. A., and Leach, J. K. (2021). Alginate-Based Bioinks for 3D Bioprinting and Fabrication of Anatomically Accurate Bone Grafts. *Tissue Eng. A* 27 (17–18), 1168–1181. doi:10.1089/ten.TEA.2020.0305

Gopalakrishnan, D. (2006). Alginate Fibres – An Overview. Available at: http://www.fibre2fashion.com/industry-article/591/alginate-fibres-an-overview (Accessed January 31, 2022).

Gopinathan, J., and Noh, I. (2018). Recent Trends in Bioinks for 3D Printing. *Biomater. Res.* 22, 11. doi:10.1186/s40824-018-0122-1

Gwon, S. H., Yoon, J., Seok, H. K., Oh, K. H., and Sun, J.-Y. (2015). Gelation Dynamics of Ionically Crosslinked Alginate Gel with Various Cations. *Macromol. Res.* 23 (12), 1112–1116. doi:10.1007/s13233-015-3151-9

Jessop, Z. M., Al-Sabah, A., Gao, N., Kyle, S., Thomas, B., Badiei, N., et al. (2019). Printability of Pulp Derived crystal, Fibril and Blend Nanocellulose-Alginate Bioinks for Extrusion 3D Bioprinting. *Biofabrication* 11 (4), 045006. doi:10.1088/1758-5090/ab0631

Kim, M. H., Lee, Y. W., Jung, W.-K., Oh, J., and Nam, S. Y. (2019). Enhanced Rheological Behaviors of Alginate Hydrogels with Carrageenan for Extrusion-Based Bioprinting. *J. Mech. Behav. Biomed. Mater.* 98, 187–194. doi:10.1016/j.jmbbm.2019.06.014

Kyburz, K. A., and Anseth, K. S. (2015). Synthetic Mimics of the Extracellular Matrix: How Simple is Complex Enough? Ann. *Biomed. Eng.* 43, 489–500. doi:10.1007/s10439-015-1297-4

Lee, J., Hong, J., Kim, W., and Kim, G. H. (2020). Bone-derived dECM/alginate Bioink for Fabricating a 3D Cell-Laden Mesh Structure for Bone Tissue Engineering. *Carbohydr. Polym.* 250, 116914. doi:10.1016/j.carbpol.2020.116914

Lee, K. Y., and Mooney, D. J. (2012). Alginate: Properties and Biomedical Applications. *Prog. Polym. Sci.* 37 (1), 106–126. doi:10.1016/j.progpolymsci.2011.06.003

Lee, P., and Rogers, M. A. (2012). Effect of Calcium Source and Exposure-Time on Basic Caviar Spherification Using Sodium Alginate. *Int. J. Gastronomy Food Sci.* 1 (2), 96–100. doi:10.1016/j.ijgfs.2013.06.003

Li, N., Guo, R., and Zhang, Z. J. (2021). Bioink Formulations for Bone Tissue Regeneration. *Front. Bioeng. Biotechnol.* 9, 44. doi:10.3389/fbioe.2021.630488

Liu, X., Yuk, H., Lin, S., Parada, G. A., Tang, T. C., Tham, E., et al. (2018). 3D Printing of Living Responsive Materials and Devices. *Adv. Mater.* 30 (4), 1704821. doi:10.1002/adma.201704821

Ma, F., Chen, C., Zheng, L., Zhou, C., Cai, K., and Han, Z. (2013). Effect of High Pressure Processing on the Gel Properties of Salt-Soluble Meat Protein Containing CaCl2 and κ-carrageenan. *Meat Sci.* 95 (1), 22–26. doi:10.1016/j.meatsci.2013.04.025

Mancha Sánchez, E., Gómez-Blanco, J. C., López Nieto, E., Casado, J. G., Macías-García, A., Díaz Díez, M. A., et al. (2020). Hydrogels for Bioprinting: A Systematic Review of Hydrogels Synthesis, Bioprinting Parameters, and Bioprinted Structures Behavior. *Front. Bioeng. Biotechnol.* 8, 776. doi:10.3389/fbioe.2020.00776

Malda, J., Visser, J., Melchels, F. P., Jüngst, T., Hennink, W. E., Dhert, W. J. A., et al. (2013). 25th Anniversary Article: Engineering Hydrogels for Biofabrication. *Adv. Mater.* 25 (36), 5011–5028. doi:10.1002/adma.201302042

Mancini, F., and McHugh, T. H. (2000). Fruit-alginate Interactions in Novel Restructured Products. *Nahrung* 44 (3), 152–157. doi:10.1002/1521-3803(20000501)44:3<152::aid-food152>3.0.co;2-8

Mandrycky, C., Wang, Z., Kim, K., and Kim, D.-H. (2016). 3D Bioprinting for Engineering Complex Tissues. *Biotechnol. Adv.* 34 (4), 422–434. doi:10.1016/j.biotechadv.2015.12.011

Merakchi, A., Bettayeb, S., Drouiche, N., Adour, L., and Lounici, H. (2018). Cross-linking and Modification of Sodium Alginate Biopolymer for Dye Removal in Aqueous Solution. *Polym. Bull.* 76 (76), 3535–3554. doi:10.1007/s00289-018-2557-x

Müller, M., Öztürk, E., Arlov, Ø., Gatenholm, P., and Zenobi-Wong, M. (2017). Alginate Sulfate-Nanocellulose Bioinks for Cartilage Bioprinting Applications. *Ann. Biomed. Eng.* 45 (1), 210–223. doi:10.1007/s10439-016-1704-5

Murphy, S. V., and Atala, A. (2014). 3D Bioprinting of Tissues and Organs. *Nat. Biotechnol.* 32 (8), 773–785. doi:10.1038/nbt.2958

Murphy, S. V., De Coppi, P., and Atala, A. (2020). Opportunities and Challenges of Translational 3D Bioprinting. *Nat. Biomed. Eng.* 4 (4), 370–380. doi:10.1038/s41551-019-0471-7

Nie, L., Wang, C., Deng, Y., and Shavandi, A. (2020). Bio-Inspired Hydrogels via 3D Bioprinting, Biomimetics. *IntechOpen*. doi:10.5772/intechopen.94985

Penman, A., and Sanderson, G. R. (1972). A Method for the Determination of Uronic Acid Sequence in Alginates. *Carbohydr. Res.* 25 (2), 273–282. doi:10.1016/s0008-6215(00)81637-7

Poldervaart, M. T., Wang, H., van der Stok, J., Weinans, H., Leeuwenburgh, S. C. G., Öner, F. C., et al. (2013). Sustained Release of BMP-2 in Bioprinted Alginate for Osteogenicity in Mice and Rats. *PLoS One* 8 (8), e72610. doi:10.1371/journal.pone.0072610

Qin, Y. (2008). Alginate Fibres: An Overview of the Production Processes and Applications in Wound Management. *Polym. Int.* 57, 171–180. doi:10.1002/pi.2296

Ramiah, P., du Toit, L. C., Choonara, Y. E., Kondiah, P. P. D., and Pillay, V. (2020). Hydrogel-Based Bioinks for 3D Bioprinting in Tissue Regeneration. *Front. Mater.* 7, 76. doi:10.3389/fmats.2020.00076

Reddy, S., and Pandit, A. (2016). Mass Transfer Characteristics of Sodium Alginate (SA) and Lignosulphonic Acid (LS) Blends. *Orient. J. Chem.* 32 (5), 2785–2790. doi:10.13005/ojc/320553

Schütz, K., Placht, A.-M., Paul, B., Brüggemeier, S., Gelinsky, M., and Lode, A. (2017). Three-dimensional Plotting of a Cell-Laden Alginate/methylcellulose Blend: towards Biofabrication of Tissue Engineering Constructs with Clinically Relevant Dimensions. *J. Tissue Eng. Regen. Med.* 11 (5), 1574–1587. doi:10.1002/term.2058

Singh, B., Sharma, V., and Chauhan, D. (2010). Gastroretentive Floating Sterculia-Alginate Beads for Use in Antiulcer Drug Delivery. *Chem. Eng. Res. Des.* 88, 997–1012. doi:10.1016/j.cherd.2010.01.017

Stokke, B. T., Draget, K. I., Smidsrød, O., Yuguchi, Y., Urakawa, H., and Kajiwara, K. (2000). Small-Angle X-ray Scattering and Rheological Characterization of Alginate Gels. 1. Ca−Alginate Gels. *Macromolecules* 33 (5), 1853–1863. doi:10.1021/ma991559q

Tabriz, A. G., Hermida, M. A., Leslie, N. R., and Shu, W. (2015). Three-dimensional Bioprinting of Complex Cell Laden Alginate Hydrogel Structures. *Biofabrication* 7 (4), 045012. doi:10.1088/1758-5090/7/4/045012

Unagolla, J. M., and Jayasuriya, A. C. (2020). Hydrogel-based 3D Bioprinting: A Comprehensive Review on Cell-Laden Hydrogels, Bioink Formulations, and Future Perspectives. *Appl. Mater. Today* 10, 100479. doi:10.1016/j.apmt.2019.100479

Urbanova, M., Pavelkova, M., Czernek, J., Kubova, K., Vyslouzil, J., Pechova, A., et al. (2019). Interaction Pathways and Structure-Chemical Transformations of Alginate Gels in Physiological Environments. *Biomacromolecules* 20 (11), 4158–4170. doi:10.1021/acs.biomac.9b01052

Wang, J., Mignon, A., Snoeck, D., Wiktor, V., Van Vliergerghe, S., Boon, N., et al. (2015). Application of Modified-Alginate Encapsulated Carbonate Producing Bacteria in concrete: a Promising Strategy for Crack Self-Healing. *Front. Microbiol.* 6, 1088. doi:10.3389/fmicb.2015.01088

Wüst, S., Godla, M. E., Müller, R., and Hofmann, S. (2014). Tunable Hydrogel Composite with Two-step Processing in Combination with Innovative Hardware Upgrade for Cell-Based Three-Dimensional Bioprinting. *Acta Biomater.* 10 (2), 630–640. doi:10.1016/j.actbio.2013.10.016

Wypych, G. (2017). "Typical Methods of Quality Control of Plasticizers," in *Handbook of Plasticizers*. Editor G. Wypych. Third Edition (Toronto, Canada: ChemTec Publishing), 85–109. doi:10.1016/B978-1-895198-97-3.50005-6

Xiong, Y. L., and Blanchard, S. P. (1993). Viscoelastic Properties of Myofibrillar Protein-Polysaccharide Composite Gels. *J. Food Sci.* 58 (1), 164–167. doi:10.1111/j.1365-2621.1993.tb03235.x

Yao, J., Zhou, Y., Chen, X., Ma, F., Li, P., and Chen, C. (2018). Effect of Sodium Alginate with Three Molecular Weight Forms on the Water Holding Capacity of Chicken Breast Myosin Gel. *Food Chem.* 239, 1134–1142. doi:10.1016/j.foodchem.2017.07.027

Conflict of Interest: Author SS is employed by Atelerix Ltd.

The remaining authors declare that the research was conducted in the absence of any commercial or financial relationships that could be construed as a potential conflict of interest.

Publisher's Note: All claims expressed in this article are solely those of the authors and do not necessarily represent those of their affiliated organizations, or those of the publisher, the editors and the reviewers. Any product that may be evaluated in this article, or claim that may be made by its manufacturer, is not guaranteed or endorsed by the publisher.